IOPscience iopscience.iop.org

Home Search Collections Journals About Contact us My IOPscience

The temperature dependence of the interband critical points in silicon within a fractional-dimensional space approach

This article has been downloaded from IOPscience. Please scroll down to see the full text article.

2004 J. Phys.: Condens. Matter 16 3041

(http://iopscience.iop.org/0953-8984/16/18/005)

View the table of contents for this issue, or go to the journal homepage for more

Download details:
IP Address: 129.252.86.83
The article was downloaded on 27/05/2010 at 14:34

Please note that terms and conditions apply.

INSTITUTE OF PHYSICS PUBLISHING JOURNAL OF PHYSICS: CONDENSED MATTER

J. Phys.: Condens. Matter **16** (2004) 3041–3051 PII: S0953-8984(04)68810-2

The temperature dependence of the interband critical points in silicon within a fractional-dimensional space approach

Keyu Tao, Tianshu Lai, Yueli Zhang, Zhaoxian Yu and Dang Mo[1]

State Key Laboratory of Optoelectronic Materials and Technologies, Department of Physics, Zhongshan (Sun Yat-Sen) University, Guangzhou 510275, People's Republic of China

E-mail: taokeyu@hotmail.com and mokdon@hotmail.com (Dang Mo)

Received 10 September 2003, in final form 3 March 2004
Published 23 April 2004
Online at stacks.iop.org/JPhysCM/16/3041
DOI: 10.1088/0953-8984/16/18/005

Abstract

The fractional-dimensional space approach (FDSA) is used to analyse the temperature dependence of direct interband transitions in Si. The critical point (CP) parameters are obtained. The results obtained by the FDSA show general or even better agreement with the theoretical calculation than the standard treatment. In the temperature range of 20–450 °C, the results obtained by FDSA indicate that the excitonic effects can be ignored, and the CP $E_1 - E_0'$ can be treated as a band character. Our research shows that the FDSA provides a good way to derive basic information on relevant physical quantities from the observed optical spectra, and it has the advantages of directness, flexibility, and sensitivity, which enable us to obtain the CP parameters efficiently without ambiguity. This method is especially useful in the cases where the limitations of the standard treatment are serious.

1. Introduction

The analysis of optical spectra provides rich information about the physical properties of materials. The dielectric function, which expresses the optical responses of materials under an external field, has been widely used for this purpose.

The structure observed in the dielectric function spectrum, which is attributed to interband critical point (CP) transitions, can be analysed in terms of the following line shape of an integer-dimensional model [1, 2]:

$$\varepsilon(E) = C - A\mathrm{e}^{\mathrm{i}\Phi}(E - E_\mathrm{g} + \mathrm{i}\Gamma)^{n/2-1} \tag{1}$$

[1] Author to whom any correspondence should be addressed.

 © 2004 IOP Publishing Ltd Printed in the UK

where the CP is described by the threshold energy E_g, broadening Γ, amplitude A, and the excitonic phase angle Φ. The parameter n is the dimensionality of this CP, which is an integer between 0 and 3. The above analytic expression provides the well-known standard treatment for analysing a critical point transition. Other typical analytic line shapes for optical spectra can be obtained from the harmonic-oscillator model [3] and more extended versions thereof [4–6].

The above methods have been widely used in the CP analysis from optical spectra. However, they have some limitations. First, in order to extract all the CP parameters, a model line shape must be assumed with regard to a chosen segment of the spectrum which contains the structure of interest. The need to assume a model line shape in advance remains a fundamental limitation because the line shape may actually be different from that of the model employed [7]. Sometimes, an inappropriate assumption may even lead to mistaken results [8, 9]. Secondly, the second or third derivative of a spectrum is generally employed to enhance a CP structure. However, differentiation also enhances noise, and the smoothing technique needed thereafter may distort the informational content of the data [7]. Thirdly, all the CP parameters are determined by minimizing the mean square deviation between the model line shape and the spectral segment. In the standard treatment, when the actual dimensionality of a CP is fractional, e.g. 1.5, both 1D and 2D models may show comparable fitting results by least-squares regression. In such a case, it is difficult to decide which model is more reasonable, let alone to find appropriate model-dependent parameters. Faced with these difficulties, some authors even present fitting results of different models without making a decision [10, 11].

Lately the fractional-dimensional space approach [12–16] (FDSA) has been acknowledged as a powerful tool to deal with intermediate-dimensional, namely fractional-dimensional, cases. In the past decade, this method has been successfully used in modelling exciton and the absorption spectra in semiconductor quantum wells, quantum well wires and superlattices [17–22]. This technique has also been used to study biexcitons [23–25], exciton–phonon interactions [26], the Stark shift of excitonic complexes [27], the refractive index [28], impurity states [29–31], the Pauli blocking effect [32], and the polaron effect [33] in quantum wells. This approach works by treating an anisotropic interaction in a three-dimensional space as an effective isotropic one in a lower-order space of fractional dimension α. The value of α is determined by the degree of the anisotropy, reflecting the mean confinement that an excitation 'feels' in the actual physical system.

We have also used the FDSA to study direct interband transitions in SiGe alloys [36]. Because of the advantages of directness, flexibility, and sensitivity in FDSA, we discovered a weak structure at the edge of the optical spectrum and a residual oxide overlayer effect.

In this paper, we apply the FDSA to the temperature dependence of interband critical points in silicon. The results are compared with those obtained by the standard treatment [34] and by microscopic calculations [11, 35] based on electron–photon and electron–phonon interaction. Our result of CP energies is in general agreement with those in the literature. With regard to lifetime broadening, better agreement with the theoretical calculation is obtained. It is shown that in the temperature range 20–450 °C, the excitonic effects can be ignored for Si, and the CP $E_1 - E_0'$ can be treated as a band character above room temperature, which is contrary to a popular viewpoint of the excitonic character of E_1. Direct evidence is also given that the CP E_2 is a much stronger structure than $E_1 - E_0'$.

This paper is organized as follows. In section 2, we give a brief description of the FDSA in direct interband transitions. In section 3 we show the results of our investigation on the temperature dependence of critical points in Si, and discuss them.

2. The fractional-dimensional space approach in direct interband transitions

By applying the fractional-dimensional space model to the optical transitions near a critical point, He and Mo have introduced the following analysis forms for treating the interband transitions [13–15]:

$$\varepsilon(E) = \frac{\mathrm{i}^{r-\alpha}\Gamma(2-\alpha/2)M_\alpha}{E^2}\int^{E-E_g+\mathrm{i}\Gamma} t^{\alpha/2-2}\,\mathrm{d}t, \tag{2}$$

where the symbols have the same meaning as in equation (1). In addition, r is the type of the CP, which is equal to the number of negative principal components of the mass tensor [1], α is the dimensionality (usually fractional) of the CP, and $M_\alpha = 2|\langle v|a\cdot p|c\rangle|^2(e/m)^2(m_{vc}/2\pi)^{\alpha/2}\hbar^{2-\alpha}/\varepsilon_0$. Since the Lorentzian broadening has been proved to be good enough in temperature-dependent studies of a number of semiconductors including Si [34, 37, 38], we also adopt it in this work.

Note that the above expression is equivalent to equation (1) when α is the integer n. So the FDSA can be thought of as evolving from the standard treatment to include the fractional-dimensional cases. After differentiating equation (1) to an order of $\alpha/2$ with respect to E [15, 39], and considering different types of CP, we find equation (2) gives, when r is even,

$$\left|\frac{\mathrm{d}^{\alpha/2}}{\mathrm{d}E^{\alpha/2}}(E^2\varepsilon_1)\right| = M_\alpha\frac{|E_g-E|}{(E_g-E)^2+\Gamma^2} = f_1, \tag{3}$$

$$\left|\frac{\mathrm{d}^{\alpha/2}}{\mathrm{d}E^{\alpha/2}}(E^2\varepsilon_2)\right| = M_\alpha\frac{\Gamma}{(E_g-E)^2+\Gamma^2} = f_2; \tag{4}$$

and when r is odd,

$$\left|\frac{\mathrm{d}^{\alpha/2}}{\mathrm{d}E^{\alpha/2}}(E^2\varepsilon_1)\right| = f_2, \tag{5}$$

$$\left|\frac{\mathrm{d}^{\alpha/2}}{\mathrm{d}E^{\alpha/2}}(E^2\varepsilon_2)\right| = f_1. \tag{6}$$

We present figure 1 to demonstrate the meaning of equations (3)–(6). Generally speaking, when the differentiation order is half the dimensionality of a CP, the corresponding segment in the derivative spectrum of the dielectric functions becomes Lorentzian line shaped, as shown in figure 1. The maximum of f_2 corresponds to the symmetric centre E_g and the amplitude Am. When E is equal to E_g plus or minus Γ, f_2 intersects with f_1, and reaches half-height of the peak ($Am/2$). The zero point of f_1 also corresponds to the symmetry centre E_g. Thus this figure allows us to directly extract all the CP parameters, avoiding complex calculations. The procedure for applying the fractional-dimensional space approach is described in the following section.

3. Result and discussion

We employ the fractional-dimensional space approach (FDSA) to investigate the temperature dependence of the critical point parameters of Si between 20 and 450 °C in the photon energy range from 1.5 to 4.7 eV. The database is from [40].

In order to make clear our procedure of applying the FDSA, the specific case of Si at 20 °C may serve as a helpful example. Our first step is to differentiate numerically [15, 39] both $(E^2\varepsilon_1)$ and $(E^2\varepsilon_2)$ of Si at 20 °C to an order of x with respect to the photon energy E, where x is increased quasi-continually from 0 to 3/2, noting that a dimensionality less than

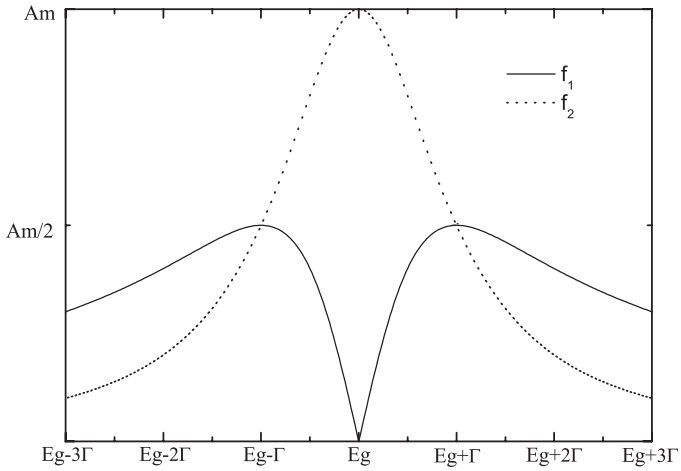

Figure 1. The Lorentzian line shape in the derivative spectra, with a differentiation order of half the dimensionality of the critical point.

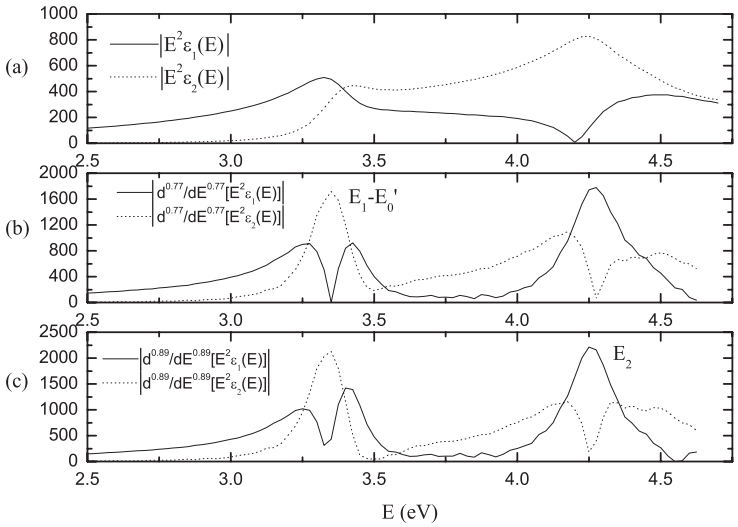

Figure 2. (a) The original spectrum of $E^2\varepsilon(E)$ of Si at 20 °C. (b) Its derivative spectrum under the differentiation order of 0.77. (c) Its derivative spectrum under the differentiation order of 0.89.

zero or greater than three has no physical meaning. The results of using different values of x are plotted in their own respective figures. Figure 2(a) is the original spectrum of $|E^2\varepsilon|$ of Si at 20 °C, which can actually be treated as the zero-order derivative. As we increase the differentiation order x, the line shapes near a critical point are asymmetric at first, then become symmetric and then asymmetric again (but in the opposite direction) until they finally deteriorate. So it is easy to find out the symmetric profile as in figure 1 from this process. For instance, figure 2(b) shows a Lorentzian line shape structure between 3 and 3.5 eV, which is identified as the CP $E_1 - E_0'$ [34, 35, 38], and figure 2(c) displays another CP structure E_2 [34, 35, 38] between 4.0 and 4.5 eV. (It might be noticed that there is some abnormality

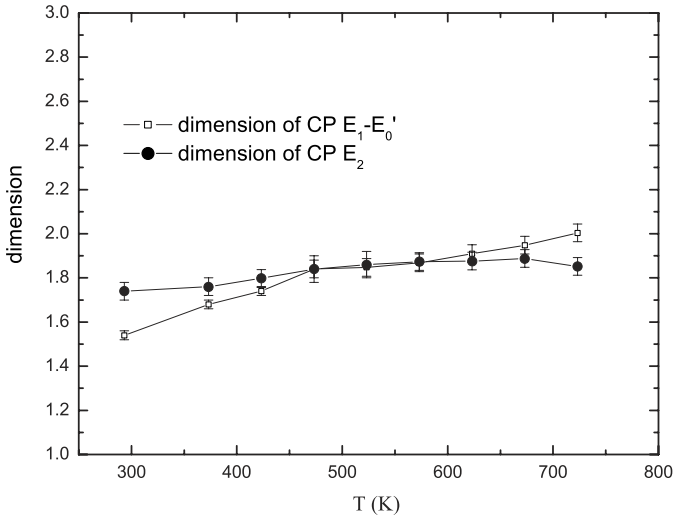

Figure 3. The temperature dependence of the dimension of the critical points for Si.

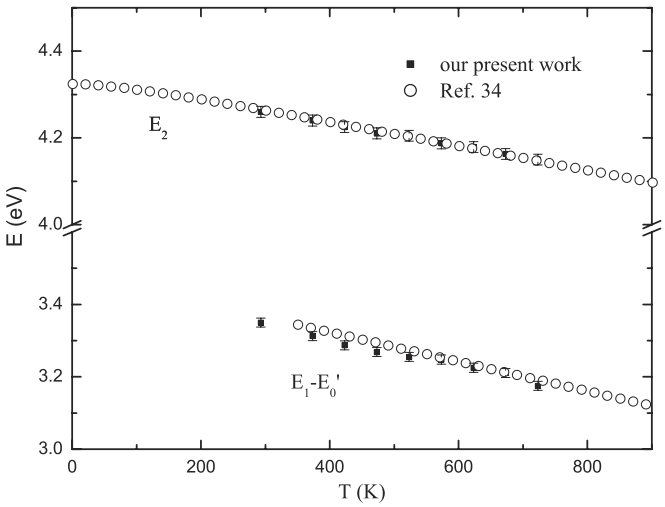

Figure 4. The temperature dependence of the interband critical point energies of Si.

in the right-hand shoulder of the CP E_2, which we will explain later in section 3.2.) Then all the transition parameters can be obtained from figure 2(b) for the CP $E_1 - E_0'$ and from figure 2(c) for the CP E_2. The dimensionality of the respective CPs is twice the differentiation order of the corresponding figure. The symmetric centre corresponds to the threshold energy E_g. The lifetime broadening Γ is the half-width at half-height. The height of the peak is the amplitude Am, and the interband momentum matrix element related parameter, $M\alpha$, equals Am multiplied by the broadening parameter Γ. All our results for the CPs $E_1 - E_0'$ and E_2 in Si are plotted in figures 3–6.

Generally speaking, the dimensionality of a CP represents the degree of the average anisotropic electron–lattice interactions during the CP transitions. It is the intrinsic property of the physical interactions. So there should, in principle, exist only one fractional dimensionality

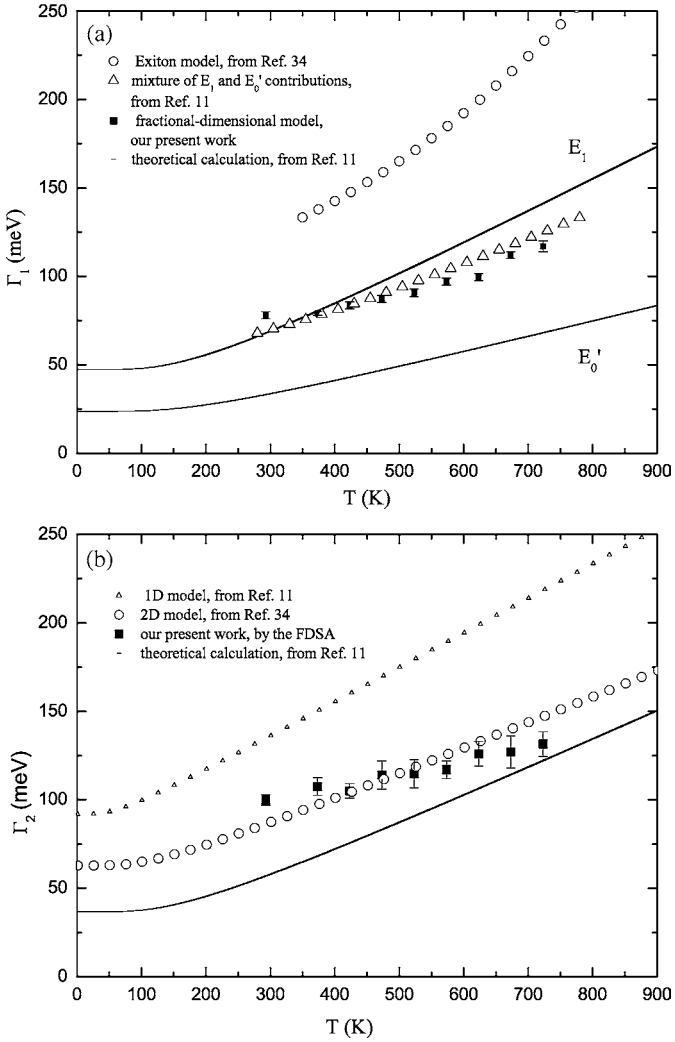

Figure 5. (a) The temperature dependence of the broadenings of the critical point $E_1 - E_0'$ for Si. Our present work (solid squares) obtained by the FDSA is compared to two different models (the excitonic (circles) and the mixture (triangles) models) in the standard treatment and theoretical calculations. (b) The temperature dependence of the broadenings of the critical point E_2 for Si. Our present work (solid squares) obtained by the FDSA is compared to two different models (1D (triangles) and 2D (circles) models) in the standard treatment and theoretical calculations.

to give a symmetric differentiated spectrum for each critical point. We can also understand this point from the physical image of the FDSA and the above application procedure. On the one hand, as can be seen from equations (3) to (6), the right-hand side of the equations (f_1 or f_2) has specific values for each critical point; on the other hand, the left-hand side (the derivative spectrum of dielectric functions) changes irreproducibly with the differentiation order (also shown in figure 2). As a result, there is only one order of differentiation (half the dimensionality) for the solution.

In early work some researchers simply assigned the peak structures of the real or imaginary part of a dielectric function to an expected critical point [41]. Later work showed that this is not necessarily true. It was realized that in neither ε_1 nor ε_2 does the maximum correspond

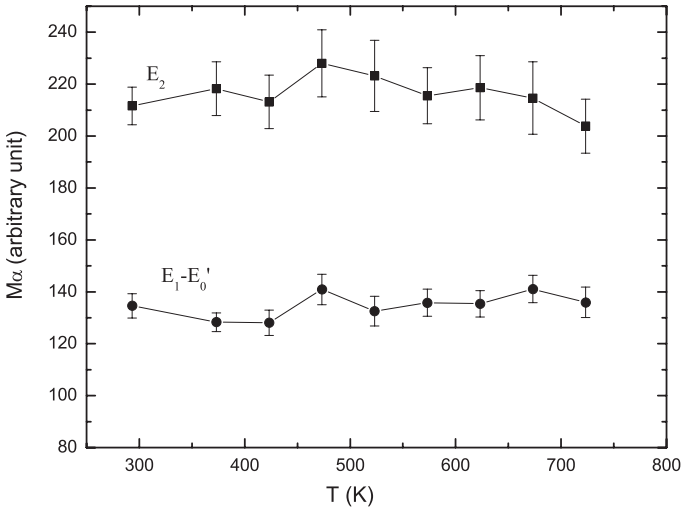

Figure 6. The temperature dependence of the interband momentum matrix related parameter $M\alpha$, defined in equation (2), measured for the CPs of Si.

to the real value of the CP energy for a nonsymmetric structure [34]. This conclusion is very natural from the viewpoint of the FDSA. In the case where the dimensionality of a CP is zero, the structure in the dielectric spectrum is symmetric, and its maximum does correspond to the CP energy [42]; however, in a more general case where the dimensionality of a CP is not zero, the structure in the original dielectric spectrum is not symmetric, and the FDSA is needed to transfer it into a symmetric one, whose maximum then corresponds to the CP energy.

It might be argued that due to the influence of other nearby CPs and noise, the actual symmetric structures shown in figure 2 are not as perfect as the ideal one shown in figure 1. In fact, the standard treatment and the other line shape fitting methods also suffer from this interference. However, it can be reduced to a large extent by the FDSA. First, the differentiation order is half the dimensionality of this CP, thus it enhances the CP structure of interest and depresses others with different dimensionality. Second, all CP parameters are determined within a comparatively small energy range from $(E_g - \Gamma)$ to $(E_g + \Gamma)$, where the character of the oscillator is prominent and less influenced by other critical points, as seen in figures 1 and 2. Our research presented in this work as well as another on the compositional dependence of $Si_{1-x}Ge_x$ [36] show that the results obtained by the FDSA are in reasonable agreement with the literature, yet remain free from tedious calculations.

3.1. The critical point $E_1 - E_0'$

The structure observed between 3.0 and 3.5 eV in the spectra (e.g., figure 2(b)) is attributed to two kinds of transition [34]. The first is the E_1 transitions taking place along the Λ directions of the Brillouin zone (BZ), and the second is the lowest direct energy gap located at the Γ point, which is labelled E_0'. The CPs E_1 and E_0' are almost degenerate and can be resolved at lower temperatures below 280 K [11]. In our research they appear as one structure from 20 to 450 °C.

It is well known that electrons endure forces introduced by the lattice in a CP transition, and the anisotropic electron–lattice interactions result in restricted, confined non-3D dynamical behaviours even in bulk material, like Si in this research. The dimensionality of a CP

characterizes the average confinement an electron experiences during the CP transitions. Figure 3 thus describes how the average confinement is affected by temperature in Si. Due to the different symmetry of corresponding points in k space for different CPs, it is not surprising that the dimensionalities of different CPs are not necessarily the same, and may change unexpectedly with temperature. As can be seen from figure 3, the dimensionality of the CP $E_1 - E_0'$ is very different from that of the CP E_2. We can also see from figure 3 that, as the confinement for the CP $E_1 - E_0'$ weakens with increasing temperature, the dimensionality increases slightly from 1.5 to 2. It is not new that the dimension of a CP can increase with temperature. GaAs, for example, was reported to display an excitonic character (0D) up to 300 K but a band character (2D) at higher temperature [37]. Unfortunately, in the standard treatment, because only integer-dimensional models are available, the dimensionality of the CP has to jump from 0 to 2 at some turning point (such as 300 K) in the case of GaAs. This limitation is avoided by the FDSA, thanks to the flexibility of the fractional dimensionality. Moreover, like the other CP parameters, the dimensionality is not an input parameter but an output one determined directly from the optical spectrum, so it can sensitively reflect the change of band structures with temperature. We note that the values (1.5–2) are quite different from the excitonic model (0) used in [34] for the CP $E_1 - E_0'$. We will return to this point later.

A comparison between our results on the temperature shift of the $E_1 - E_0'$ gap and those of [34] is shown in figure 4. Our results obtained by the FDSA are plotted with solid squares. The results of [34], obtained by the standard treatment, are plotted with circles. We can see that the agreement is reasonable, and the maximum deviation is less than 0.81% for the CP $E_1 - E_0'$. Moreover, we can also see good agreement for the CP E_2. Since both our results and the ones from [34] have overlapping margins of error and can therefore be considered virtually the same, we do not discuss their comparison with the theoretical calculation [35] here. Interested readers can refer to [34] and [35].

With regard to the lifetime broadenings Γ_1, figure 5(a) shows the comparison of our result obtained by the FDSA with those obtained by different integer-dimensional models in the standard treatment [11, 34], and those obtained by theoretical calculation [11]. It is obvious that our result is in good agreement with the one obtained by the model considering a mixture line shape of 2D and excitonic, noting the contribution from E_0' and E_1 [11]. The broadenings of both results are basically between the theoretical E_0' and E_1 curves, and they are much closer to the theoretical E_1 curve. The agreement is sound, as it is already known that the contribution of E_1 is dominant in the combined transitions [11, 34]. However, the broadenings obtained from the pure excitonic model [34], which are represented by the circle symbols in figure 5(a), seem 1.5–2 times bigger than the above results. Such a large discrepancy from the theoretical result is unlikely to be attributed to the electron–electron interaction and surface scattering indicated by [34]. It is known that the lifetime broadening parameter is dependent on the dimensional models used in the standard treatment [10, 34]. Generally speaking, the smaller the dimensionality of a model, the bigger the lifetime broadening. So it is not surprising that the excitonic model yields substantially greater broadening than the mixture model of 2D and 0D, as demonstrated in figure 5(a). Moreover, it was found recently that a pure excitonic line shape was not suitable for describing the dielectric behaviour near the CP $E_1 - E_0'$ of Si [38]. Instead, Aoki and Adachi [38] also employed a 2D model combining excitonic effects at low temperatures, which greatly improved the fit of the dielectric function of Si in the temperature range 30–793 K.

The theoretical calculations shown in figure 5 are based on a phonon-induced broadenings mechanism [11]. In such a mechanism, temperature dependence of lifetime broadenings is caused by the electron–phonon interaction, which shortens the lifetime of electronic states and thus increases the lifetime broadening with increasing temperature. Since the agreements

between our results obtained by the FDSA and the theoretical calculations based on electron–phonon interaction are quite satisfying, no other interaction is artificially needed to explain the broadening phenomena.

Furthermore, Lautenschlager *et al* [34] have investigated the character of E_1 transitions in semiconductors (IV) and compounds (III–V, II–VI). Their results are given in table 3 of [34]. The regularity they found is that the higher the high-frequency dielectric constant ($\varepsilon(\infty)$), the less the localized character. However, it should be noticed that the regularity is systematic except for Si. In the excitonic area of the table, all the constants ($\varepsilon(\infty)$) are basically less than 10, while the $\varepsilon(\infty)$ of Si is 12, which is apparently greater than 9.6 (InP) and 10.9 (GaAs) in the 2D area. If we treat E_1 in Si not as a pure excitonic but as a band characteristic critical point, the regularity of the table appears more reasonable and satisfying.

Although excitonic effects were introduced to overcome the difficulties of the underestimated intensity of E_1 in *ab initio* calculations [43, 44], our results obtained from experimental data, combined with Adachi's work [38], seem to indicate that in the temperature range of 20–450 °C the excitonic effects can be ignored, and the simple model of the FDSA in our paper, which is within the framework of the one-electron approximation, provides a good description of band character for the CP $E_1 - E_0'$ in Si. However, when the temperature becomes very low, the contribution of the excitonic effects must be considered in the FDSA model to give a proper explanation for the spectral change [5, 38].

3.2. The critical point E_2 transitions

The higher energy critical point between 4.0 and 4.5 eV in figure 2(c) is labelled E_2 [34], and is attributed to several transitions in the band. Their origins in the Brillouin zone (BZ) are not well defined, and they are usually attributed to the area including or near the X and Σ points in k space [34, 38]. This indicates that the small abnormality in the right-hand shoulder of the symmetric structure for E_2 in figure 2(c) is caused by the superposition of close CPs with different dimensionality, amplitude and broadenings. However, as an approximation, we ignore this abnormality and treat them as one structure; the results are still satisfying and agree well with both the analysis results of the experiment in [34] and the theoretical calculus of [35].

The temperature dependence of the dimensionality of the CP E_2 is also demonstrated in figure 3. It is clear that in the temperature range 20–450 °C the dimensionality of the CP E_2 is between 1.7 and 1.9, which can be reasonably simplified as a 2D model in the standard treatment [34].

As indicated by figure 4, the temperature dependence of the E_2 energy gap agrees well with [34], and the deviation is less than 0.2%. For the reason mentioned in section 3.1, we do not discuss it further.

Figure 5(b) shows the temperature dependence of the lifetime broadening for the CP E_2. From this figure we can see that our result agrees with that obtained by the 2D model [34], but is much lower than that of the 1D model [11]. This is reasonable. Since the dimensionality for the CP E_2 is between 1.7 and 1.9, the 2D model is a good approximation, while the 1D model clearly yields much larger Γ. As for the comparison of experimental results with theoretical ones, there is still a discrepancy (figure 5(b)). This is because the origin of the E_2 structure in the optical spectra is not well-defined in the BZ, as mentioned above. It is attributed to transitions in several regions, while the theoretical curve plotted in figure 5(b) only concerns transitions at the point $(2\pi/a_0)$ (0.9, 0.1, 0.1) [11]. In addition, the local pseudopotential band structure for theoretical calculus underestimates the E_2 CP energies by about 10%, which leads to a lower electronic density of states and as a result comparatively lower values for the broadening parameters.

The parameter $M\alpha$, which is proportional to $|\langle v|a\cdot p|c\rangle|^2$, can be obtained from the equality $M\alpha = Am \times \Gamma$. We plot this parameter as a function of temperature in figure 6. It is almost independent of temperature, which suggests that the band structure does not undergo a notable change in the temperature range 20–450 °C. This figure also shows that the values of $M\alpha$ for E_2 are much larger than those for $E_1 - E_0'$, which provides direct evidence that the CP E_2 is a much stronger structure than the CP $E_1 - E_0'$ [34].

4. Conclusion

The temperature dependence of the dielectric function of Si was analysed in the 1.5–4.7 eV photon energy range from 20 to 450 °C. By performing the FDSA on the observed structures, the parameters (dimensionality, threshold energy and lifetime broadening) of the critical points $E_1 - E_0'$ and E_2 were obtained. These results are compared with those obtained by the standard treatment and theoretical calculations. With regard to energy shift, good agreement is achieved. The broadening obtained by the FDSA agrees better with the theoretical calculation. Our results show that in the temperature range 20–450 °C, the excitonic effects can be ignored and the CP $E_1 - E_0'$ can be described by a band character. Direct evidence is provided that E_2 is a stronger structure than $E_1 - E_0'$.

Our research including this work and another on SiGe alloys [36] demonstrates that the FDSA can avoid the limitations within the previous methods mentioned in section 1. First, the FDSA can be used to obtain all the CP parameters directly from the optical spectrum without tedious calculation. No assumption or adjustable parameter is needed. Second, the order of differentiation in the FDSA is no greater than 3/2, which is much smaller than the differentiation order of 2 or 3 generally required by the standard treatment, thus reducing the need for smoothing techniques; this preserves the integrity of the experimental data. Third, the FDSA is flexible enough to deal with any integer- or fractional-dimensional critical points with one unified model. Moreover, since all the CP parameters are not adjustable parameters but are extracted directly from the optical spectrum, they are as sensitive as the optical spectrum itself, reflecting small changes in the band structure due to composition, temperature, stress or other conditions. Because of all these advantages, we anticipate that the FDSA can be generally applied to other semiconductors for CP analysis in the optical spectrum, especially in the cases where the limitations of the previous methods are serious.

Acknowledgments

The authors are grateful to Dr Haichao Zhang for helpful discussion about the theoretical calculation of phonon-induced lifetime broadenings. The authors are also grateful to Alexandre Elias for carefully reading this manuscript. This work is supported by the National Natural Science Foundation of China (under Grant No. 50372085) and by SRF for ROCS, SEM.

References

[1] Aspnes D E 1980 *Handbook on Semiconductors* vol 2, ed M Balkanski (Amsterdam: North-Holland) p 109
Cardona M 1969 *Modulation Spectroscopy* (*Solid State Physics Suppl. 11*) ed F Seitz, D Turnbull and H Ehrenreich (New York: Academic)
[2] Yu P Y and Cardona M 1996 *Fundamentals of Semiconductors* (Berlin: Springer)
[3] Martin B G and Wallis R F 1977 *Solid State Commun.* **21** 385
Erman M, Theeten J B, Chambon P, Kelso S M and Aspnes D E 1984 *J. Appl. Phys.* **56** 2664
[4] Kim C C, Garland J W and Raccah P M 1993 *Phys. Rev.* B **47** 1876
[5] Adachi S 1987 *Phys. Rev.* B **35** 7454
Adachi S 1990 *Phys. Rev.* B **41** 1003

[6] Herzinger C M, Johs B, McGahan W A, Woollam J A and Paulson W 1998 *J. Appl. Phys.* **83** 3323
[7] Lastras-Martínez L F, Ruf T, Konuma M, Cardona M and Aspnes D E 2000 *Phys. Rev.* B **61** 12946
[8] Carlos Y and Ming L 1998 *Thin Solid Films* **313/314** 237
Loo R, Caymax M, Libezny M, Blavier G, Brijs B, Geenen L and Vandervorst W 2000 *J. Electrochem. Soc.* **147** 751
[9] Pollak F H 2000 *J. Appl. Phys.* **88** 2175
[10] Vina L, Logothetidis S and Cardona M 1984 *Phys. Rev.* B **30** 1979
[11] Lautenschlager P, Allen P B and Cardona M 1986 *Phys. Rev.* B **33** 5501
[12] Herrick D R and Stillinger F H 1975 *Phys. Rev.* A **11** 42
Stillinger F H 1977 *J. Math. Phys.* **18** 1224 and references therein
[13] He X-F and Mo D 1986 *Chin. Phys. Lett.* **3** 565
[14] He X-F 1987 *Solid State Commun.* **61** 53
[15] He X-F 1990 *Phys. Rev.* B **42** 11751
[16] He X-F 1991 *Phys. Rev.* B **43** 2063
[17] Lefebvre P, Christol P, Mathieu H and Glutsch S 1995 *Phys. Rev.* B **52** 5756
[18] Zhao Q X, Monemar B, Holtz P O, Willander M, Fimland B O and Johannessen K 1994 *Phys. Rev.* B **50** 4476
[19] Lefebvre P, Christol P and Mathieu H 1993 *Phys. Rev.* B **48** 17308
[20] Lefebvre P, Christol P and Mathieu H 1992 *Phys. Rev.* B **46** 13603
[21] Mathieu H, Lefebvre P and Christol P 1992 *Phys. Rev.* B **46** 4092
[22] Christol P, Lefebvre P and Mathieu H 1993 *J. Appl. Phys.* **74** 5626
[23] Thilagam A 1997 *Phys. Rev.* B **55** 7804
[24] Mizeikis V, Birkedal D, Langebein W, Lyssenko V G and Hvam J M 1997 *Phys. Rev.* B **55** 5284
[25] Birkedal D, Singh J, Lyssenko V G, Erland J and Hvam J M 1996 *Phys. Rev. Lett.* **76** 672
[26] Thilagam A 1997 *Phys. Rev.* B **56** 9798
[27] Thilagam A 1997 *Phys. Rev.* B **56** 4665
[28] Tanguy C, Lefebvre P, Mathieu H and Elliot R J 1997 *J. Appl. Phys.* **82** 798
[29] Mikhailov I D, Betancur F J, Escorcia R A and Sierra-Ortega J 2003 *Phys. Rev.* B **67** 115317
[30] Reyes-Go'mez E, Oliveira L E and de Dios-Leyva M 1999 *J. Appl. Phys.* **85** 4045
[31] Reyes-Go'mez E, Matos-Abiague A, Perdomo-Leiva C A, de Dios-Leyva M and Oliveira L E 2000 *Phys. Rev.* B **61** 13104
[32] Thilagam A 1999 *Phys. Rev.* B **59** 3027
[33] Matos-Abiague A 2002 *Phys. Rev.* B **65** 165321
[34] Lautenschlager P, Garriga M, Vina L and Cardona M 1987 *Phys. Rev.* B **36** 4821
[35] Lautenschlager P, Allen P B and Cardona M 1985 *Phys. Rev.* B **31** 2163
[36] Tao K Y, Zhang Y L, Mo D, Sano N and Kaneko T 2003 *J. Appl. Phys.* **94** 3995
[37] Lautenschlager P, Garriga M, Logothetidis S and Cardona M 1987 *Phys. Rev.* B **35** 9174
[38] Aoki T and Adachi S 1991 *J. Appl. Phys.* **69** 1574
[39] Oldham K B and Spanier J 1974 *The Fractional Calculus* (New York: Academic)
Ross B (ed) 1975 *Fractional Calculus and Its Applications* (Berlin: Spinger)
[40] Vuye G, Fisson S, Nguyen V, Wang Y, Rivory J and Abeles F 1993 *Thin Solid Films* **233** 166
[41] Jellison G E Jr and Modine F A 1983 *Phys. Rev.* B **27** 7466
[42] Muñoz M, Huang Y S, Pollak F H and Yang H 2003 *J. Appl. Phys.* **93** 2549
[43] Hanke W and Sham L J 1979 *Phys. Rev. Lett.* **43** 387
[44] Albrecht S, Reining L, Del Sole R and Onida G 1998 *Phys. Rev. Lett.* **80** 4510